Glycative Stress Research

Online edition : ISSN 2188-3610
Print edition : ISSN 2188-3602
Received : August 22, 2022
Accepted : September 14, 2022
Published online : September 30, 2022
doi:10.24659/gsr.9.3_175

Original article

Antiglycative effect of extract and phenolic compounds from holy basil (*Ocimum tenuiflorum*)

Kento Kunihiro [1, 2], Tai Kaneshima [3], Takao Myoda [3]

1) Graduate School of Bioindustry, Tokyo University of Agriculture, Hokkaido, Japan
2) Albion Co. Ltd., Tokyo, Japan
3) Department of Food, Aroma and Cosmetic Chemistry, Tokyo University of Agriculture, Hokkaido, Japan

Abstract

***Aim*:** Glycation reactions involve the binding of sugars to amino groups of proteins to form advanced glycation end products (AGEs) via glycation intermediates. AGEs induce inflammatory and protein dysfunctions, leading to diabetes and skin aging. The aim of this study was to evaluate the anti-glycation effect of holy basil (*Ocimum tenuiflorum*) leaf extract and identify the compounds responsible for these effects.

***Methods*:** The crude extract was obtained by hot water extraction of dried holy basil leaves. The total polyphenol and flavonoid contents and antioxidant activities of the crude extract were determined. Phenolic compounds were isolated from the crude extract using various chromatographic methods. The effect of the crude extract and isolated compounds on the formation of fluorescent AGEs, N^{ε}-(carboxymethyl) lysine (CML), 3-deoxyglucosone (3-DG), glyoxal (GO), and methylglyoxal (MGO) were examined.

***Results*:** The crude extract of holy basil was rich in polyphenols, most of which were flavonoids. Luteolin 5-*O*-glucoside (**1**), luteolin 7-*O*-glucuronide (**2**), (–)-rabdosiin (**3**), apigenin 7-*O*-glucuronide (**4**), rosmarinic acid (**5**), globoidnan A (**6**), and salvianolic acid A (**7**) isolated from the crude extract inhibited the formation of fluorescent AGEs, CML, 3-DG, GO, and MGO. In particular, compounds **3**, **5**, **6**, and **7** were potent antiglycation compounds. The crude extract also showed high antioxidant activities.

***Conclusions*:** Phenolic compounds of holy basil were found to be the active components endowing antiglycative effects. One of the antiglycation mechanisms of these polyphenols could be related to the antioxidant action of holy basil.

***KEY WORDS*:** antiglycative effect, advanced glycation end products (AGEs), holy basil (*Ocimum tenuiflorum*), polyphenols

Introduction

Glycation is a non-enzymatic reaction between reducing sugars and amino groups in proteins, lipids, and nucleic acids and produces advanced glycation end products (AGEs) [1]. Accumulation of AGEs, such as N^{ε}-(carboxymethyl) lysine (CML), in dermal tissue influences glycation stress in the skin. AGEs partially accumulate in the skin by binding to collagen proteins. Lysine and arginine, the amino acids in collagen, can be glycated to AGEs to form crosslinks between glycated collagen. Glycation of collagen induces skin aging, leading to the loss of skin elasticity and wrinkle formation [2]. Glycation is an aging process related to oxidative stress and is also associated with diabetic complications, atherosclerosis, neuropathies, and Alzheimer's disease [3, 4]. Furthermore, diseases caused by the glycation reaction *in vivo* result from oxidative and inflammatory stresses due to reactive oxygen species, which induce structural and functional protein alterations, cellular dysfunction, apoptosis, and organ injuries [5]. Thus, glycation is associated with various diseases and aging. Therefore, inhibition of glycation is important for protection against aging and for maintaining homeostasis.

The genus *Ocimum*, belonging to the family Labiatae, consists of 30 species that are distributed in tropical and subtropical regions. Holy basil (*Ocimum tenuiflorum*) has traditionally been used in India and Sri Lanka for the

Correspondence author: Tai Kaneshima, PhD
Department of Food, Aroma and Cosmetic Chemistry, Tokyo University of Agriculture
196 Yasaka, Abashiri-shi, Hokkaido 099-2493, Japan
TEL: +81-152-48-3871 FAX: +81-152-48-2531 e-mail: tk203897@nodai.ac.jp
Co-authors: Kunihiro K, k_kunihiro@albion.co.jp; Myoda T, t1myouda@nodai.ac.jp

treatment of various diseases. This plant is used to prepare herbal tea or dried powder and treat colds, headaches, coughs, heart disease, and skin diseases [6]. A previous study suggested that the essential oils of holy basil leaves have potent antioxidant activity [7]. Holy basil also contains many non-volatile compounds, including saponins, flavonoids, and tannins [8]. Zhao *et al*. showed that polyphenols, i.e. protocyanidins, condensed tannins, and flavonoids, play an important role in antiglycation activity [9]. Holy basil can be expected to have a high inhibitory effect on glycation because phenolic compounds such as luteolin, apigenin, orientin, eugenol, caffeic acid, and rosmarinic acid have been reported as the main bioactive constituents [10, 11]. The aim of this study was to evaluate the antiglycative effect of the extract from holy basil leaves, quantify the phenolic compounds and their antioxidant activities, and investigate the formation of fluorescent AGEs, CML, and glycation intermediates.

Material and methods

1) Chemicals and reagents

Gallic acid, methanol (MeOH), Folin-Ciocalteu reagent, sodium hydroxide (NaOH), (+)-catechin, sodium nitrite, aluminum trichloride, acetic acid, sodium acetate trihydrate, methanol-d_4 (MeOD), potassium persulfate, acetonitrile, formic acid, rosmarinic acid, salvianolic acid A, glucose, sodium hydrogen phosphate, sodium dihydrogen phosphate, aminoguanidine, 2,3-butanedione, perchloric acid, sodium hydrogen carbonate, 2,3-diaminonaphthalene, ethyl acetate, glyoxal (GO), methylglyoxal (MGO) and ethanol (EtOH) were purchased from Fujifilm Wako Pure Chemicals (Osaka, Japan). 1,1-Diphenyl-2-picrylhydrazyl (DPPH), 2,2'-azino-bis (3-ethylbenzothiazoline-6-sulfonic acid) (ABTS), and bovine serum albumin (BSA) were obtained from Sigma Aldrich (St. Louis, USA). 3-deoxyglucosone (3-DG) was purchased from Dojindo Laboratory (Kumamoto, Japan). Luteolin 5-*O*-glucoside, luteolin 7-*O*-glucronide, and apigenin 7-*O*-glucronide were purchased from Namiki Shoji (Tokyo, Japan). (–)-Rabdosiin was obtained from MedChemExpress (NJ, USA).

2) General experimental methods

The UV (ultra violet) spectra were acquired on a V-570 UV/Vis spectrometer (Jasco, Tokyo). ^{1}H and ^{13}C nuclear magnetic resonance (NMR) spectra were recorded on a ECZ-600 spectrometer (JEOL, Tokyo) at 600 and 125 MHz, respectively. Chemical shifts are expressed in δ (ppm) and referenced to the residual solvent peaks. The optical rotations were measured using a Jasco P-1030 instrument. High-performance liquid chromatography (HPLC) was performed on a Jasco LC-2000 Plus HPLC system equipped with an MD-2010 Plus photodiode array (PDA) detector and an Atlantis T3 column (3 μm, 150 mm × 4.6 mm i.d., Waters, Milford, MA, USA) using an acetonitrile-H_2O-formic acid solvent system. Mass spectra were obtained using liquid chromatography time-of-flight mass spectrometry (LC-TOF-MS). The LC-TOF-MS was performed on an Agilent 1200 Infinity HPLC and Agilent 6540 Agilent Ultra-High-Definition Accurate-Mass Q-TOF LC/MS instrument. The mass spectra were recorded in the negative electrospray ionization (ESI) mode. Preparative HPLC was performed using a LC-8A pump (Shimadzu, Kyoto, Japan), UV-4570 detector (Jasco), and Inertsil ODS-4 column (3 μm, 250 mm × 20 mm i.d., GL Sciences, Tokyo). The samples were eluted at a flow rate of 6.0 mL/min using 20% ~ 27% acetonitrile containing 0.1% acetic acid as a mobile phase. Signals were recorded at 280 nm.

3) Plant materials and extraction

Holy basil (*Ocimum tenuiflorum*) fresh leaves were collected in a medicinal garden at the Institute of Traditional Plants (Negombo, Sri Lanka). The seedlings were purchased from the Department of Agriculture (Peradeniya, Sri Lanka) under the Ministry of Agriculture, which identified by the Industrial Technology Institute (Colombo, Sri Lanka). Then, the plant was cultivated for at least six months. The collected leaves were washed, and dried at 25°C and 50% ~ 70% humidity for two weeks. The dried leaves of holy basil (50 g) were extracted with distilled water (500 mL) at 100°C for 1 h. Then, the extract was filtered, evaporated, and lyophilized to obtain the crude extract (11.6 g).

4) Determination of total polyphenol content

The total polyphenol content was determined using the Folin-Ciocalte method [12]. The crude extract was adjusted to 0.5 mg/mL with 50% MeOH and used as the sample solution. The sample solution (20 μL) was mixed with 1 N Folin-Ciocalteu reagent (40 μL). Then, 1 N NaOH (100 μL) was added to the mixture and incubated for 15 min, followed by centrifugation at 20,000 × g and 4°C for 5 min. The supernatant was dispensed into 96 well plate, and the absorbance was measured at 734 nm using a microplate reader (SpectraMax i3x, Molecular Devices, CA, USA). The total polyphenol content was expressed as mg gallic acid equivalents/g of the sample. The assays were performed in triplicate.

5) Determination of total flavonoid content

The total flavonoid content was determined using the aluminum chloride colorimetric assay [13]. The crude extract was adjusted to 0.5 mg/mL with 50% MeOH and used as the sample solution. The sample solution (125 μL) was mixed with 5% sodium nitrite (40 μL) and distilled water (625 μL) and incubated for 5 min. Next, 10% aluminum trichloride (250 μL) was added and incubated for 6 min, followed by the addition of 1 N NaOH (250 μL) and distilled water (140 μL). The mixture was vortexed and the absorbance at 510 nm was measured using a microplate reader. The total flavonoid content was expressed as mg (+)-catechin equivalents per gram of the sample. The assays were performed in triplicate.

6) 1,1-Diphenyl-2-picrylhydrazyl (DPPH) radical scavenging assay

The DPPH radical scavenging activity was measured as reported previously [7]. The crude extract was adjusted to 1 ~ 100 μg/mL with 50% MeOH and used as the sample solution. The sample solution (40 μL) was mixed with 100 mM acetate

buffer (40 μL, pH 5.5), and then a 0.5 mM DPPH• solution in EtOH (20 μL) was added. The reaction mixture was vortexed and incubated in the dark for 30 min at 30 °C, after which the absorbance was measured at 517 nm (A_{517}) using a microplate reader. The DPPH radical scavenging activity was calculated using the following equation:

DPPH radical scavenging activity (%)
= [(A_{517} (control) – A_{517} (sample)) / A_{517} (control)] × 100

IC_{50} (50% inhibitory concentration) values were calculated from the percentage decrease relative to the sample concentration. The assays were performed in triplicate. Gallic acid and ascorbic acid were used as positive controls.

7) 2,2'-Azino-bis (3-ethylbenzothiazoline-6-sulfonic acid) (ABTS) radical cation scavenging assay

The ABTS radical cation scavenging activity was measured as reported previously [7]. First, 10 mL of 7 mM ABTS• solution was mixed with 176 μL of 140 mM potassium persulfate, and the mixture was allowed to stand in the dark at 25 °C for 12 ~ 16 h. The solution was then diluted 30-fold with EtOH, and the absorbance of this ABTS• solution at 734 nm was measured to be approximately 0.700 using a spectrophotometer. The crude extract was adjusted to 1 ~ 200 μg/mL with 50% MeOH and used as the sample solution. The sample solution (20 μL) was then added to the ABTS• solution (200 μL). The mixture was vortexed and incubated for 4 min at 37 °C, following which the absorbance was read at 734 nm (A_{734}) using a microplate reader. The ABTS radical cation scavenging activity was calculated using the following equation:

ABTS radical cation scavenging activity (%)
= [(A_{734} (control) – A_{734} (sample)) / A_{734} (control)] × 100

IC_{50} values were calculated from the percentage decrease relative to the sample concentration. The assays were performed in triplicate. Gallic acid and ascorbic acid were used as positive controls.

8) Superoxide dismutase (SOD)-like activity

The SOD-like activity was evaluated using the SOD Assay Kit-WST (Dojindo Laboratory, Kumamoto, Japan) according to the protocol. The crude extract was adjusted to 1 ~ 50 μg/mL with 50% MeOH and used as the sample solution. The sample solution (20 μL) and 200 μL of WST working solution were mixed with enzyme working solution (20 μL). The mixture was vortexed and incubated for 20 min at 37 °C, following which the absorbance was read at 450 nm (A_{450}) using a microplate reader. The antioxidant activity was expressed as the percentage inhibition, as follows:

Inhibition (%)
= [(A_{450} (control) – A_{450} (sample)) / A_{450} (control)] × 100

IC_{50} values were calculated from the percentage decrease relative to the sample concentration. The assays were performed in triplicate. Gallic acid and ascorbic acid were used as positive controls.

9) Isolation of phenolic compounds

The crude extract (8.0 g) was dissolved in distilled water and applied to a DIAION HP-20 column (Mitsubishi Chemical, Tokyo; 35 g; 330 mm × 30 mm i.d.) equilibrated with distilled water. The column was eluted with a H_2O-MeOH solvent system (300 mL) and three fractions, namely, H_2O Fr. (5.40 g), 50% MeOH Fr. (1.84 g), and 100% MeOH Fr. (0.50 g), were obtained. The 50% MeOH Fr. sample (1.0 g) was further separated on a Sephadex LH-20 column (Cytiva Sweden AB, Upsala, Sweden; 25 g; 300 mm × 30 mm i.d.) using H_2O/MeOH mixture (100:0, 75:25, 50:50, 25:75, and 0:100 v/v; 200 mL). The fractions collected using 25% ~ 100% MeOH were dissolved in 20% ~ 27% acetonitrile, and the soluble portion was subjected to preparative HPLC. Seven phenolic compounds were isolated from each of the fractions. Among the seven compounds, compound **1** (6.1 mg) was isolated from 75% MeOH Fr., compound **2** (66.3 mg), **3** (7.1 mg), **4** (6.8 mg), and **5** (23.8 mg) were isolated from 25% MeOH Fr., and compound **6** (6.2 mg) and **7** (3.5 mg) were isolated from the 100% MeOH fraction. The purities of the isolated compounds were confirmed by HPLC. The structures of compounds **1** ~ **7** (***Fig. 1***) obtained from the crude extract were analyzed by LC-TOF-MS, ^{1}H NMR spectroscopy, ^{13}C NMR spectroscopy, UV spectroscopy, and specific optical rotation measurement. Compounds were identified by a direct comparison of the HPLC chromatograms with those of the standards.

10) Preparation of glycated proteins

The glycated proteins were prepared in accordance with a previously reported method [14]. The BSA-glucose glycation model was used to investigate the effect of the crude extract of holy basil and the compounds isolated from it upon glycation. BSA was added to a final concentration of 10 mg/mL to a 100 mg/mL glucose solution prepared in 0.1 M phosphate-buffered saline (PBS, pH 7.2), and the mixture was incubated at 60 °C for seven days (solution A). As a background, a 10 mg/mL BSA solution without glucose was prepared (solution B). To clarify the effects of the crude extract and isolated compounds, samples of the indicated concentrations were added to the reaction mixture in the presence or absence of glucose (solutions C and D, respectively). Aminoguanidine was used as a positive control. Aliquots of the reaction mixtures were then assayed for the formation of AGE and AGE intermediates. The reaction mixtures were kept at −20 °C until analysis.

11) Measurement of AGE-derived fluorescence

AGE formation was measured using a fluorescence microplate reader at excitation and emission wavelengths of 370 and 440 nm, respectively [15]. The inhibitory activity against fluorescent AGE formation of the crude extract, isolated compound, and aminoguanidine was calculated as following equation and the IC_{50} values also were obtained from the plot of the inhibitory activity relative to the sample concentration.

Inhibitory activity of fluorescent AGE formation (%)
= {[fluorescence of (solution A – solution B) – (solution C – solution D)] / fluorescence of (solution A – solution B)} × 100

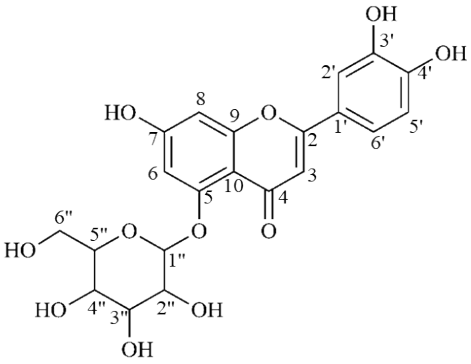

Luteolin 5-*O*-glucoside (**1**)

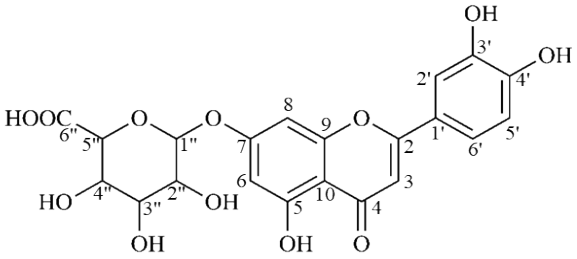

Luteolin 7-*O*-glucronide (**2**)

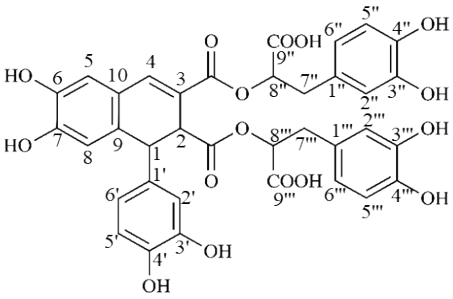

(–)-Rabdosiin (**3**)

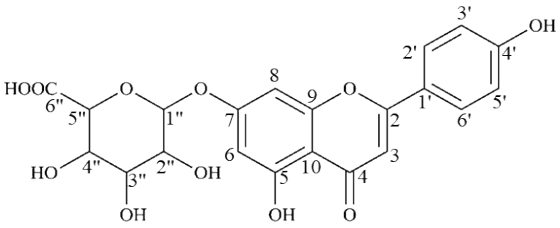

Apigenin 7-*O*-glucronide (**4**)

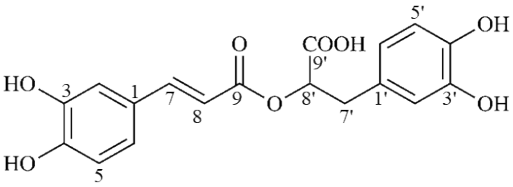

Rosmarinic acid (**5**)

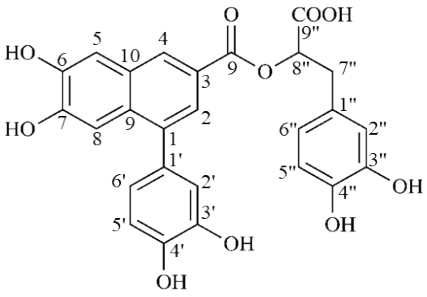

Globoidnan A (**6**)

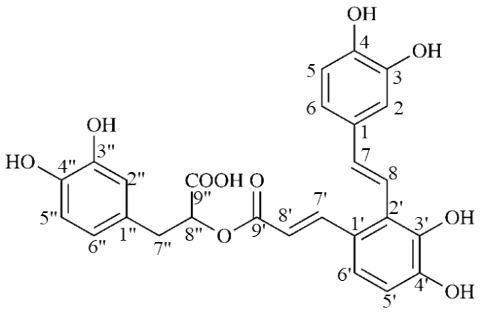

Salvianolic acid A (**7**)

Fig. 1. **Chemical structures of the phenolic compounds isolated from holy basil.**

12) Measurement of CML

CML is a non-fluorescent AGE and the most abundant product of the glycation reaction. CML produced in the reaction mixtures was quantified by ELISA (enzyme-linked immuno sorbent assay) using the CircuLex CML/N^{ε}-(carboxymethyl) lysine ELISA Kit (Medical and Biological Laboratories, Tokyo, Japan), following the manufacturer's instructions. To prepare the test solution, the reaction mixture was diluted 250-fold with 0.1 M PBS. The CML content showed as the percentage of CML formation compared to that of controls without sample addition.

13) Measurement of AGE intermediates

3-DG, GO, and MGO were identified as intermediates of the AGEs using a high-performance liquid chromatography-ultraviolet (HPLC-UV) system, as reported previously [16]. Samples were prepared by adding 50 µL aliquots of the reaction mixtures to 6 µL of 5 µg/mL 2,3-butanedione, which was used as an internal standard, and 75 µL of distilled water. The mixture was vortexed, following which 125 µL of 6.0% perchloric acid was added. Then, the mixture was centrifuged at 12,000 × g for 10 min. The supernatant was added to 125 µL of saturated sodium hydrogen carbonate and 12.5 µL of 1 mg/mL 2,3-diaminonaphthalene labeling reagent. The mixture was incubated overnight at 4 °C. The next day, ethyl acetate (0.5 mL) was added to the reaction solution for liquid-liquid extraction, followed by centrifugation at 1,000 × g for 10 min. The supernatant was concentrated by distillation under a nitrogen atmosphere. Subsequently, 100 µL of MeOH was added, and the mixture was used as the sample for analysis. The standards for 3-DG, GO, and MGO were analyzed by HPLC using an Inertsil ODS-3 column (5 µm, 150 mm × 4.6 mm i.d., GL Sciences). The mobile phase for gradient elution was as follows: solvent A: H_2O, solvent B: 100% acetonitrile. The gradient conditions were as follows: 0 min, 10% B; 55 min, 41.4% B. The flow rate and detection wavelength were 1.0 mL/min and 268 nm, respectively.

Statistical analysis

All statistical analyses were performed using GraphPad Prism 5 for Windows (GraphPad Software, San Diego, CA). Values are expressed as mean ± standard deviation (SD). Statistical analysis was performed using one-way ANOVA followed by Tukey's test for statistical comparisons among groups, with a value of $p < 0.05$ indicating significance.

Results

Total polyphenol and flavonoid contents

The total polyphenol and flavonoid contents were 214.5 ± 8.0 mg gallic acid equivalents/g extract and 146.6 ± 4.6 mg catechin equivalents/g extract respectively. The results indicated that approximately 70% of the polyphenols in the crude holy basil extract were flavonoids.

Antioxidant activity

Antioxidant properties of the crude extract are listed in ***Table 1***. The crude extract showed DPPH radical scavenging activity, ABTS radical cation scavenging activity, and SOD-like activity, with IC_{50} values of 36.6 ± 0.2 µg/mL, 172.1 ± 6.5 µg/mL, and 39.5 ± 3.6 µg/mL, respectively. The IC_{50} values of the crude extract obtained in the DPPH radical and ABTS radical cation scavenging assays were approximately 30% lower than those of ascorbic acid; However, the values were approximately 4.5-fold higher in SOD-like activity.

Structure analysis of isolated compound

The crude extract of holy basil was fractionated by chromatography on DIAION HP-20 column and Sephadex LH-20 column, followed by purification by preparative HPLC to isolate phenolic compounds. Luteolin 5-*O*-glucoside (**1**), luteolin 7-*O*-glucuronide (**2**), (–)-rabdosiin (**3**), apigenin 7-*O*-glucuronide (**4**), rosmarinic acid (**5**), globoidnan A (**6**), and salvianolic acid A (**7**) were isolated (***Fig. 2***). Their compounds were identified by comparison of the data to the references [17-23]. The spectroscopic data of isolated compounds were in the Supplementary data. Although compounds **1**, **2**, **3**, **4**, and **5** have been found in various plants, compounds **6** and **7** in holy basil is being reported for the first time.

Inhibitory activity on the formation of fluorescent AGEs

The inhibitory activities of the crude extract of holy basil and the isolated compound for the formation of fluorescent AGEs are shown in ***Table 2***. Both the crude extract and isolated compounds inhibited the formation of fluorescent AGEs. Their inhibitory activity was stronger than that of aminoguanidine, which was used as a positive control. Compounds **3**, **5**, **6**, and **7** significantly suppressed the formation of fluorescent AGEs.

Table 1. Antioxidant activity of the crude extract of holy basil.

Sample	DPPH radical scavenging activity (IC_{50}; µg/mL)	ABTS radical cation scavenging activity (IC_{50}; µg/mL)	SOD-like activity (IC_{50}; µg/mL)
Crude extract	36.6 ± 0.2^{c}	172.1 ± 6.5^{c}	39.5 ± 3.6^{c}
Gallic acid	3.5 ± 0.6^{a}	12.4 ± 0.2^{a}	0.6 ± 0.3^{a}
Ascorbic acid	11.8 ± 1.0^{b}	61.8 ± 9.5^{b}	179.0 ± 1.9^{b}

Values represent mean ± SD from three independent experiments, and means within columns with the same superscript letters are not significantly different ($p < 0.05$). DPPH,1,1-diphenyl-2-picrylhydrazyl; ABTS, 2,2'-azino-bis (3-ethylbenzothiazoline-6-sulfonic acid); SOD, superoxide dismutase; IC_{50}, 50% inhibitory concentration; SD, standard deviation.

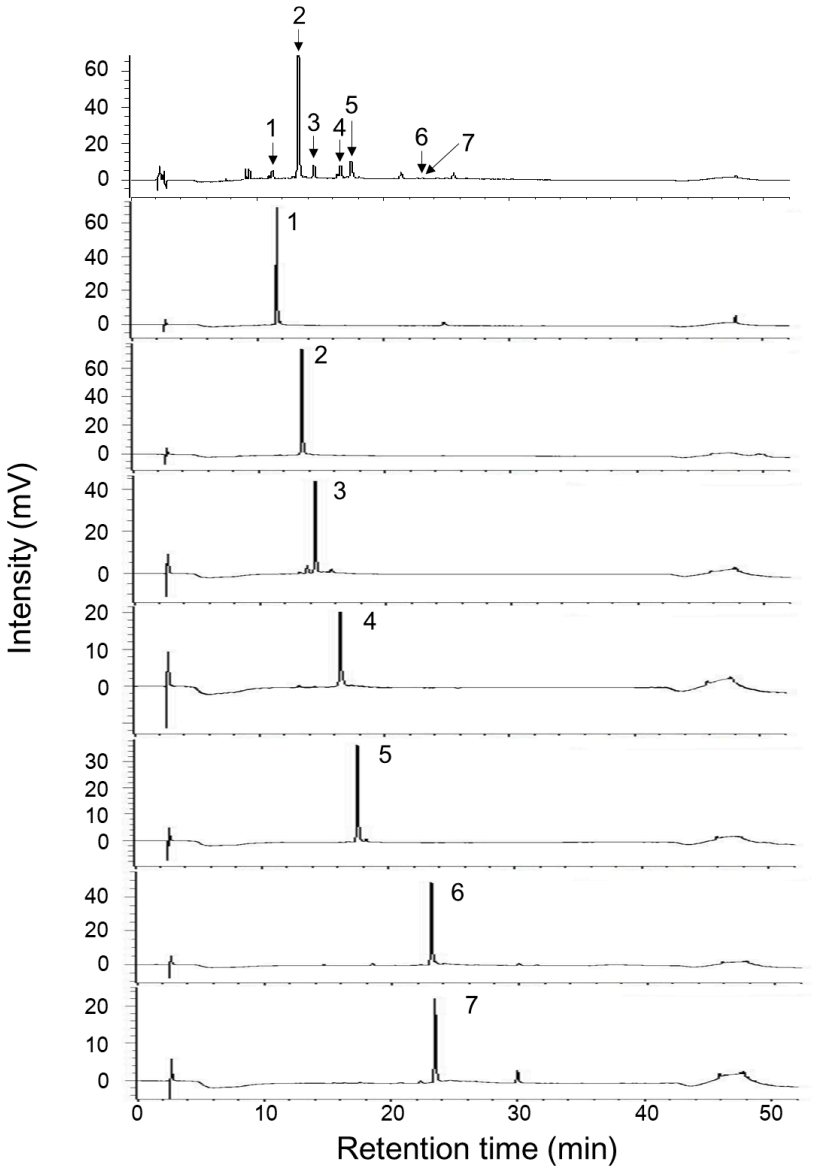

Fig. 2. **HPLC chromatogram of the phenolic compounds isolated from the crude extract of holy basil.**

Detection: PDA detector (280 nm); gradient condition: 5%～100% acetonitrile containing 0.1% formic acid. 1: Luteolin 5-*O*-glucoside (**1**), 2: Luteolin 7-*O*-glucronide (**2**), 3: (-)-Rabdosiin (**3**), 4: Apigenin 7-*O*-glucronide (**4**), 5: Rosmarinic acid (**5**), 6: Globoidnan A (**6**), 7: Salvianolic acid A (**7**). HPLC, high-performance liquid chromatography; PDA, photodiode array.

Supplementary data

Spectroscopic data of compounds **1**–**7**

Luteolin 5-*O*-glucoside (**1**): yellow amorphous powder; UV (MeOH) λ_{max} = 248, 346 nm; HR-ESI-MS *m/z* 447.0945 [M-H]$^-$, *calcd*. for $C_{21}H_{20}O_{11}$, 448.1018; ^{1}H NMR (600 MHz, MeOD): δ 7.37 (dd, 1H, *J* = 7.6, 2.0 Hz, H-6'), 7.35 (brs, 1H, H-2'), 6.89 (d, 1H, *J* = 8.2 Hz, H-5'), 6.81 (d, 1H, *J* = 2.0 Hz, H-6), 6.69 (d, 1H, *J* = 2.0 Hz, H-8), 6.52 (s, 1H, H-3), 4.83 (d, 1H, *J* = 7.6 Hz, H-1''), 3.94 (dd, 1H, *J* = 12.0, 1.4 Hz, H-6''α), 3.75 (dd, 1H, *J* = 12.0, 5.5 Hz, H-6''β), 3.58–3.60 (m, 1H, H-2''), 3.42–3.50 (m, 3H, H-3'', H-4'', H-5''); ^{13}C NMR (125 MHz, MeOD): δ 180.4 (C-4), 165.3 (C-7), 164.4 (C-2), 160.7 (C-9), 160.1 (C-5), 150.8 (C-4'), 147.0 (C-3'), 123.5 (C-1'), 120.1 (C-6'), 116.8 (C-5'), 114.0 (C-2'), 109.2 (C-10), 106.5 (C-3), 105.1 (C-1''), 104.9 (C-6), 99.3 (C-8), 78.6 (C-5''), 77.3 (C-3''), 74.7 (C-2''), 71.2 (C-4''), 62.5 (C-6''). The above data were in consistency with the reported values of Luteolin 5-*O*-glucoside (Sevindik *et al*., 2015).

Luteolin 7-*O*-glucronide (**2**): yellow amorphous powder; UV (MeOH) λ_{max} = 253, 266, 347 nm; HR-ESI-MS *m/z* 461.0729 [M-H]$^-$, *calcd*. for $C_{21}H_{18}O_{12}$, 462.0798; ^{1}H NMR (600 MHz, MeOD): δ 7.43 (d, 1H, *J* = 7.6 Hz, H-6'), 7.41 (s, 1H, H-2'), 6.90 (d, 1H, *J* = 8.3 Hz, H-5'), 6.82 (d, 1H, *J* = 2.1 Hz, H-8), 6.60 (s, 1H, H-3), 6.49 (d, 1H, *J* = 2.1 Hz, H-6), 5.10 (d, 1H, *J* = 7.6 Hz, H-1''), 3.93 (d, 1H, *J* = 9.0 Hz, H-5''), 3.53–3.57 (m, 3H, H-2'', H-3'', H-4''); ^{13}C NMR (125 MHz, MeOD): δ 184.1 (C-3), 175.0 (C-6''), 166.9 (C-2), 164.9 (C-7), 162.8 (C-5), 159.0 (C-9), 151.2 (C-4'), 147.1 (C-3'), 123.5 (C-1'), 120.5 (C-6'), 116.8 (C-5'), 114.3 (C-2'), 107.2 (C-10), 104.1 (C-3), 101.6 (C-1''), 101.4 (C-6), 96.1 (C-8), 77.5 (C-3''), 76.6 (C-5''), 74.5 (C-2''), 73.3 (C-4''). The above data were in consistency with the reported values of luteolin 7-*O*-glucronide (Bhatarrai *et al*., 2019).

(–)-Rabdosiin (**3**): light brown amorphous powder; UV (MeOH) λ_{max} = 255, 285, 345 nm; [α]D = -37.6 (c = 0.50, MeOH), HR-ESI-MS *m/z* 717.1475 [M-H]$^-$, *calcd*. for $C_{36}H_{30}O_{16}$, 718.1549; ^{1}H NMR (600 MHz, MeOD): δ 7.58 (s, 1H, H-4), 6.79 (s, 1H, H-5), 6.74 (d, 1H, *J* = 2.1 Hz, H-2''), 6.68 (d, 1H, *J* = 1.4 Hz, H-2'''), 6.66 (d, 1H, *J* = 8.2 Hz, H-5'''), 6.64 (d, 1H, *J* = 7.6 Hz, H-5''), 6.60 (d, 1H, *J* = 8.2 Hz, H-5'), 6.55 (d, 1H, *J* = 7.6 Hz, H-6''), 6.50 (d, 1H, *J* = 8.0 Hz, H-6'''), 6.49 (s, 1H, H-8), 6.35 (d, 1H, *J* = 8.2, 2.0 Hz, H-6'), 6.33 (d, 1H, *J* = 2.0 Hz, H-2'), 5.04 (dd, 1H, *J* = 7.9, 4.8 Hz, H-8'''), 4.97 (dd, 1H, *J* = 6.9, 4.8 Hz, H-8''), 4.44 (brs, 1H, H-1), 3.88 (d, 1H, *J* = 1.5 Hz, H-2), 3.03 (dd, 1H, *J* = 14.5, 4.1 Hz, H-7'''), 2.98 (dd, 1H, *J* = 13.8, 3.8 Hz, H-7'''), 2.91–2.96 (m, 2H, H-7''); ^{13}C NMR (125 MHz, MeOD): δ 174.3 (C-9'''), 173.7 (2-COO-), 173.5 (C-9'') , 168.0 (3-COO-), 149.1 (C-7), 146.1 (C-3''), 146.0 (C-3'''), 145.9 (C-4'''), 145.4 (C-6), 145.1 (C-4''), 145.1 (C-3'), 144.8 (C-4'), 140.9 (C-4), 136.8 (C-1'), 131.4 (C-9), 129.6 (C-1''), 129.5 (C-1'''), 124.7 (C-10), 122.0 (C-6'''), 121.4 (C-6''), 120.5 (C-3), 119.9 (C-6'), 117.7 (C-2'''), 117.6 (C-2''), 117.5 (C-8), 117.3 (C-5), 116.4 (C-5''), 116.3 (C-5'''), 116.3 (C-5'), 115.6 (C-2'), 75.7 (C-8''), 75.7 (C-8'''), 49.9 (C-2), 46.1 (C-1), 38.1 (C-7''), 37.7 (C-7'''). The above data were in consistency with the reported values of (–)-rabdosiin (Ozgen *et al*., 2010).

Apigenin 7-*O*-glucronide (**4**): yellow amorphous powder; UV (MeOH) λ_{max} = 235, 265, 340 nm; HR-ESI-MS *m/z* 445.0765 [M-H]$^-$, *calcd*. for $C_{21}H_{18}O_{11}$, 446.0841; ^{1}H NMR (600 MHz, MeOD): δ 7.87 (d, 2H, *J* = 7.6 Hz, H-2', H-6'), 6.92 (d, 2H, *J* = 8.3 Hz, H-3', H-5'), 6.81 (d, 1H, *J* = 1.8 Hz, H-8), 6.64 (s, 1H, H-3), 6.48 (d, 1H, *J* = 1.4 Hz, H-6), 5.13 (d, 1H, *J* = 7.6 Hz, H-1''), 4.03 (d, 1H, *J* = 8.3 Hz, H-5''), 3.53–3.60 (m, 3H, H-2'', H-3'', H-4''); ^{13}C NMR (125 MHz, MeOD): δ 184.1 (C-4), 175.6 (C-6''), 166.8 (C-2), 164.6 (C-7), 162.9 (C-5), 162.9 (C-4'), 159.0 (C-9), 129.7 (C-2'), 129.7 (C-6'), 123.1 (C-1'), 117.0 (C-3'), 117.0 (C-5'), 107.2 (C-10), 104.1 (C-3), 101.4 (C-1''), 101.2 (C-6), 96.0 (C-8), 77.3 (C-3''), 76.6 (C-5''), 74.4 (C-2''), 73.1 (C-4''). The above data were in consistency with the reported values of apigenin 7-*O*-glucronide (Moussaoui *et al*., 2010).

Rosmarinic acid (**5**): brown amorphous solid; UV (MeOH) λ_{max} = 235 and 330 nm; HR-ESI-MS *m/z* 359.0776 [M-H]$^-$, *calcd*. for $C_{18}H_{16}O_8$, 360.0845; ^{1}H NMR (600 MHz, MeOD): δ 7.54 (d, 1H, *J* = 15.8 Hz, H-7), 7.03 (d, 1H, *J* = 2.1 Hz, H-2), 6.95 (dd, 1H, *J* = 8.3, 2.0 Hz, H-6), 6.77 (d, 1H, *J* = 7.6 Hz, H-5), 6.74 (d, 1H, *J* = 1.5 Hz, H-2'), 6.68 (d, 1H, *J* = 7.6 Hz, H-5'), 6.61 (dd, 1H, *J* = 8.2, 2.1 Hz, H-6'), 6.26 (d, 1H, *J* = 16.5 Hz, H-8), 5.17 (dd, 1H, *J* = 8.3, 4.1 Hz, H-8'), 3.09 (dd, 1H, *J* = 14.5, 4.1 Hz, H-7'α), 2.99 (dd, 1H, *J* = 14.5, 8.3 Hz, H-7'β); ^{13}C NMR (125 MHz, MeOD): δ 173.7 (C-9'), 168.5 (C-9), 149.7 (C-4), 147.7 (C-7), 146.8 (C-3), 146.1 (C-3'), 145.2 (C-4'), 129.4 (C-1'), 127.2 (C-1), 123.1 (C-6), 121.8 (C-6'), 117.6 (C-2'), 116.5 (C-5), 116.3 (C-5'), 115.2 (C-2), 114.5 (C-8), 74.8 (C-8'), 37.9 (C-7'). The above data were in consistency with the reported values of rosmarinic acid (Sevindik *et al*., 2015).

Globoidan A (**6**). light brown amorphous powder; UV (MeOH) λ_{max} = 261 and 318 nm; HR-ESI-MS *m/z* 491.0987 [M-H]$^-$, *calcd*. for $C_{26}H_{20}O_{10}$, 492.1062; ^{1}H NMR (600 MHz, MeOD): δ 8.24 (brs, 1H, H-4), 7.62 (d, 1H, *J* = 1.4 Hz, H-2), 7.26 (s, 1H, H-8), 7.24 (s, 1H, H-5), 6.87 (d, 1H, *J* = 8.3 Hz, H-5'), 6.86 (d, 1H, *J* = 2.0 Hz, H-2'), 6.79 (d, 1H, *J* = 2.0 Hz, H-2''), 6.75 (dd, 1H, *J* = 8.2, 2.0 Hz, H-6'), 6.68 (dd, 1H, *J* = 8.2, 2.0 Hz, H-6''), 6.65 (d, 1H, *J* = 8.2 Hz, H-5''), 5.24 (dd, 1H, *J* = 9.6, 3.4 Hz, H-8''), 3.16 (dd, 1H, *J* = 13.4, 3.4 Hz, H-7''), 3.05 (dd, 1H, *J* = 14.5, 9.6 Hz, H-7''); ^{13}C NMR (125 MHz, MeOD): δ 174.2 (C-9''), 168.4 (C-9), 150.2 (C-7), 148.3 (C-6), 146.2 (C-4'), 146.1 (C-3'), 145.9 (C-3''), 145.2 (C-4''), 140.0 (C-1), 133.8 (C-1'), 131.9 (C-8a), 130.3 (C-1''), 129.8 (C-4a), 129.4 (C-4), 125.1 (C-3), 124.4 (C-2), 122.4 (C-6'), 121.9 (C-6''), 118.0 (C-2'), 117.6 (C-2''), 116.4 (C-5''), 116.3 (C-5'), 112.4 (C-5), 109.4 (C-8), 76.0 (C-8''), 38.2 (C-7''). The above data were in consistency with the reported values of globoidan A (D'Urso *et al*).

Salvianolic acid A (**7**): yellow amorphous powder; UV (MeOH) λ_{ma} = 227 and 287 nm; HR-ESI-MS *m/z* 493.1147 [M-H]$^-$, *calcd*. for $C_{26}H_{22}O_{10}$, 494.1220; ^{1}H NMR (600 MHz, MeOD): δ 8.02 (d, 1H, *J* = 15.8 Hz, H-7'), 7.12 (d, 1H, *J* = 16.5 Hz, H-8), 7.10 (d, 1H, *J* = 8.9 Hz, H-6'), 7.03 (d, 1H, *J* = 2.0 Hz, H-2), 6.86 (dd, 1H, *J* = 8.3, 2.0 Hz, H-6), 6.74 (d, 1H, *J* = 7.6 Hz, H-5'), 6.73 (d, 1H, *J* = 7.6 Hz, H-5), 6.71 (d, 1H, *J* = 2.1 Hz, H-2"), 6.65 (d, 1H, *J* = 15.8 Hz, H-7), 6.62 (d, 1H, *J* = 8.3 Hz, H-5"), 6.54 (dd, 1H, *J* = 8.3, 1.4 Hz, H-6"), 6.29 (d, 1H, *J* = 15.8 Hz, H-8'), 5.12 (dd, 1H, *J* = 8.3, 2.7 Hz, H-8"), 3.06 (dd, 1H, *J* = 14.5, 3.4 Hz, H-7"), 2.92 (dd, 1H, *J* = 13.8, 9.0 Hz, H-7"); ^{13}C NMR (125 MHz, MeOD): δ 175.5 (C-9"), 168.9 (C-9'), 148.2 (C-4'), 146.9 (C-7'), 146.7 (C-4), 146.4 (C-3), 146.0 (C-3"), 145.0 (C-4"), 144.4 (C-3'), 137.8 (C-7), 131.4 (C-1), 130.0 (C-1"), 128.2 (C-2'), 126.2 (C-1'), 122.0 (C-6"), 120.6 (C-8), 120.4 (C-6), 120.1 (C-6'), 117.3 (C-2"), 116.5 (C-5"), 116.3 (C-5), 116.1 (C-8'), 114.7 (C-5'), 114.0 (C-2), 76.3 (C-8"), 38.2 (C-7"). The above data were in consistency with the reported values of salvianolic acid A (Zhou *et al*., 2014).

Table 2. Inhibitory activity against fluorescent AGE formation.

Sample	IC_{50} value (mg/mL)	IC_{50} value (mM)
Crude extract	0.37 ± 0.02^b	–
Luteolin 5-*O*-glucoside (**1**)	0.22 ± 0.02^c	0.49 ± 0.05^b
Luteolin 7-*O*-glucronide (**2**)	0.25 ± 0.01^c	0.55 ± 0.01^b
(–)-Rabdosiin (**3**)	0.15 ± 0.01^d	0.21 ± 0.02^c
Apigenin 7-*O*-glucronide (**4**)	0.23 ± 0.01^c	0.52 ± 0.02^b
Rosmarinic acid (**5**)	0.07 ± 0.01^e	0.20 ± 0.04^c
Globoidnan A (**6**)	0.08 ± 0.01^e	0.16 ± 0.02^c
Salvianolic acid A (**7**)	0.09 ± 0.01^e	0.18 ± 0.03^c
Aminoguanidine	0.49 ± 0.04^a	6.74 ± 0.58^a

Values represent mean ± SD from three independent experiments, and means within columns with the same superscript letters are not significantly different ($p < 0.05$). AGE, advanced glycation end product; SD, standard deviation.

Inhibitory activity on the formation of CML and AGE intermediates

To examine the inhibitory activity for the formation of non-fluorescent AGEs, the level of CML, which is one of the AGEs, was measured using ELISA. As shown in ***Fig. 3***, the CML levels decreased in the crude extract of holy basil and the compounds isolated from it. The inhibition rates of CML formation in the crude extract, compounds **1**, **2**, and **4** were 10 % ~ 20 % lower than that of the control. Compounds **3**, **5**, **6**, and **7** were more potent in inhibiting CML formation than that of the crude extract, compounds **1**, **2**, and **4**.

Next, we evaluated the effects of the crude extract of holy basil and the compounds isolated from it on the formation of AGE intermediates (***Fig. 4***). HPLC-UV analysis revealed the formation of three types of intermediates, namely, 3-DG, GO, and MGO. Both crude extract and the isolated compounds suppressed the formation of 3-DG, GO, and MGO. In particular, compounds **3**, **5**, **6**, and **7** significantly reduced the formation of AGE intermediates. The crude extract showed approximately 30 % inhibitory activity against 3-DG formation; compounds **1**, **2**, and **4** showed approximately 50 % activity; and compounds **3**, **5**, **6**, and **7** showed the highest inhibition activities (approximately 70 %). The formation of GO and MGO was inhibited by 40 % ~ 50 % upon the addition of the crude extract, compounds **1**, **2**, and **4**; and compounds **3**, **5**, **6**, and **7** had potent inhibitory activity of AGE intermediates (approximately 60 % ~ 70 %).

Discussion

Glycation stress *in vivo* is one of the causes of aging and lifestyle-related diseases, and AGE formation by glycation is associated with oxidative reactions. Aminoguanidine inhibits AGE production; however, ingestion of the compound causes side effects such as anemia, liver damage, and vitamin B6 deficiency [24]. Therefore, new antiglycation components, such as luteolin, cyanidin 3-*O*-galactoside, and rhodanthenone B have been isolated from medicinal herbs [25-27].

Holy basil is an important herb in traditional medicines

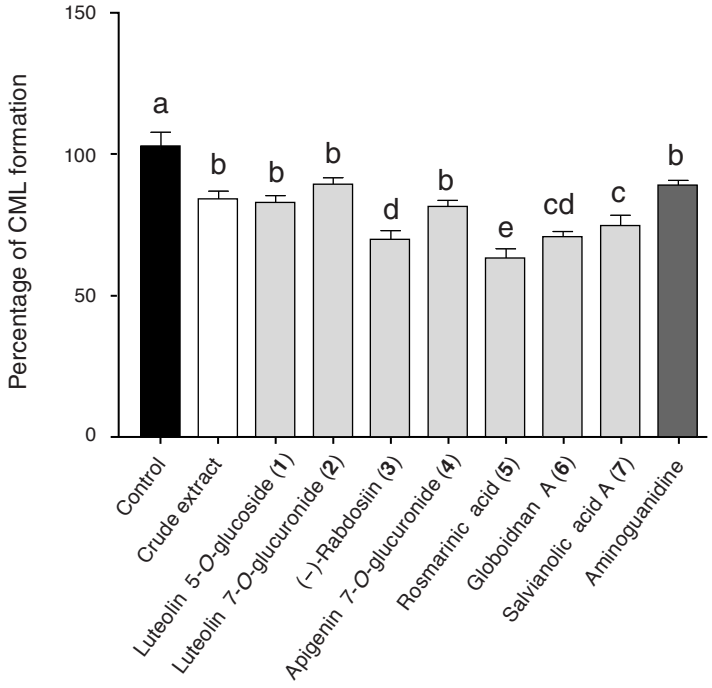

Fig. 3. **Effects of the crude extract of holy basil and the phenolic compounds isolated from it on the formation of CML.**

Extract and isolated compounds with indicated percentages were introduced into the BSA-glucose model and incubated at 60 °C for seven days. CML was quantified using ELISA. Data were calculated as the percentage of CML formation compared to that of controls without sample addition and are presented as mean ± SD (n = 8). Bar with different letters (**a** - **e**) differ ($p < 0.05$). CML, N^{ε}-(carboxymethyl) lysine; ELISA, enzyme-linked immuno sorbent assay; SD, standard deviation.

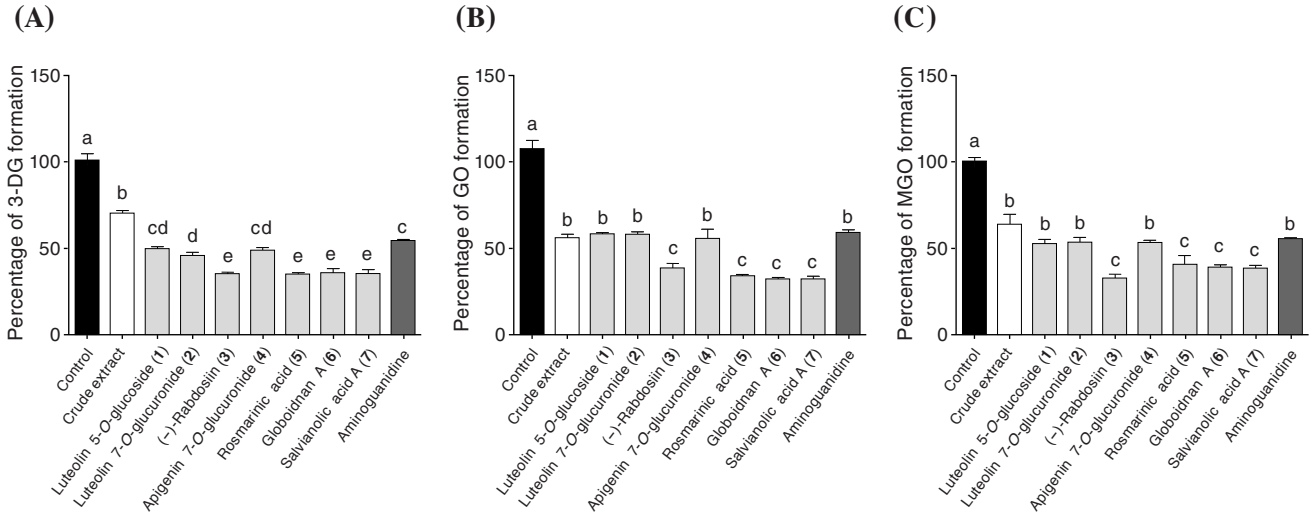

Fig. 4. **Effects of the crude extract of holy basil and the phenolic compound isolated from it on the formation of AGE intermediate.**

Extract and isolated compounds with indicated percentages were introduced into the BSA-glucose model and incubated at 60 °C for seven days. The AGE intermediates were detected using a HPLC-UV system: (**A**) 3-DG, (**B**) GO, and (**C**) MGO. Data were calculated as the percentage of AGE intermediate formation compared to that of controls without sample addition and are presented as mean ± SD (n = 3). Different letters (**a** - **e**) for the same method represent statistically significant differences between samples ($p < 0.05$). AGE, advanced glycation end product; BSA, bovine serum albumin; HPLC, high-performance liquid chromatography; UV, ultra violet; 3-DG, 3-deoxyglucosone; GO, glyoxal; MGO, methylglyoxal; SD, standard deviation.

and is often referred to as "The Queen of Herbs" or "The Incomparable One" or "The Mother Medicine of Nature in Ayurveda Systems"[28]. This herb has a history of more than 3000 years as a medicinal plant in India and Sri Lanka and has potential functional properties. In this study, the physiological functions of holy basil were evaluated using its antiglycative effect as an indicator. The hot water extract of holy basil exhibited strong antiglycation activity. The extract was mostly composed of flavonoids such as luteolin 5-*O*-glucoside (**1**), luteolin 7-*O*-glucuronide (**2**), (–)-rabdosiin (**3**), apigenin 7-*O*-glucronide (**4**), rosmarinic acid (**5**), globoidnan A (**6**), and salvianolic acid A (**7**), and these flavonoids were found to be active components for the antiglycative effect. In particular, compounds **3**, **5**, **6**, and **7** showed stronger antiglycation activities than glycosides.

Yang *et al.*[29] reported that kaempferol exhibited stronger antiglycation inhibitory activity than kaempferol glycosides in the BSA-glucose model, which is consistent with our results. Incidentally, compounds **6** and **7** have been isolated and identified in holy basil leaves for the first time. The mechanism of *in vivo* glycation involves the accumulation of AGEs due to the metabolism of dicarbonyl derivatives such GO, 3-DG, and MGO[3,30]. Among the AGEs, CML, which is generated by an intramolecular Cannizzaro reaction with GO as a precursor and by oxidative cleavage of Schiff bases or Amadori compounds, has been detected in patients with diabetes and high oxidative stress[31]. Therefore, the effect of the crude extract of holy basil and the compounds isolated from it on the glycation reaction was examined, and indeed, GO formation was significantly inhibited. This result suggested that the inhibition of GO formation led to the suppression of CML accumulation by preventing subsequent metabolism.

In a previous study, free radical scavenging was proposed as an anti-glycation mechanism[32]. The crude extract of holy basil scavenged DPPH and ABTS radical cations and also exhibited SOD-like activity. These results suggest that the antioxidant properties of holy basil help in inhibiting AGE formation. Oxidative stress plays an important role in the mechanism of AGE formation and accumulation *in vivo* and is implicated as a key factor in the progression of several diseases. Glycation, which is accelerated in the presence of oxidative stress in tissues, induces aging[33]. It has been suggested that the extract of holy basil, which has potent antioxidant activity, can be an effective component in inhibiting age-related glycation; however, further research is needed to elucidate the *in vivo* antiglycative mechanism.

Conclusions

Herein, we report the antiglycative effect of the extract of holy basil and the phenolic compounds isolated from it on the BSA-glucose system. The crude extract of holy basil is rich in polyphenols, and luteolin 5-*O*-glucoside (**1**), luteolin 7-*O*-glucuronide (**2**), (–)-rabdosiin (**3**), apigenin 7-*O*-glucuronide (**4**), rosmarinic acid (**5**), globoidnan A (**6**), and salvianolic acid A (**7**) present in it significantly inhibited the formation of fluorescent AGEs, CML, and glycation intermediates. It has been suggested that the antioxidant activity of these phenolic compounds can contribute to the antiglycation effect. Our findings showed that compounds **3**, **5**, **6**, and **7** were the active constituents of holy basil. The properties of holy basil are beneficial for the development of cosmetics, supplements, medicines, and other applications.

Acknowledgments

The authors acknowledge Ayano Kinjo for supporting this study. The publication of this study was supported by the Isyoku-Dogen Research Foundation (IDF#221001).

Conflict of interest

The authors have no conflicts of interest directly relevant to the content of this article.

References

1) Singh R, Barden A, Mori T, et al. Advanced glycation-endproducts:a review. *Diabetologia*. 2001; 44: 129-146.
2) Ichihashi M, Yagi M, Nomoto K, et al. Glycation stress and photo-aging in skin. *Anti-Aging Med*. 2011; 8: 23-29.
3) Ahmed N. Advanced glycation end products: Role in pathology of diabetic complications. *Diabetes Res Clin Pract*. 2005; 67: 3-21.
4) Takedo A, Yasuda T, Miyata T, et al. Immunohistochemical study of advanced glycation end products in aging and Alzheimer's disease brain. *Neurosci Lett*. 1996; 221: 17-20.
5) Uribarri J, Cai W, Peppa M, et al. Circulating glycotoxins and dietary advanced glycation endproducts: Two links to inflammatory response, oxidative stress, and aging. *J Gerontol A Biol Sci Med Sci*. 2007; 62: 427-433.
6) Cohen MM. Tulsi – Ocimum sanctum: A herb for all reasons. *J Ayurveda Integr Med*. 2014; 5: 251-259.
7) Kunihiro K, Kikuchi Y, Nojima S, et al. Characteristic of aroma components and antioxidant activity of essential oil from *Ocimum tenuiflorum* leaves. *Flavour & Fragrance J*. 2022; 37: 210-218.
8) Pattanayak P, Behera P, Das D, et al. *Ocimum sanctum* Linn. A reservoir plant for therapeutic applications: An overview. *Pharmacogn Rev*. 2010; 4: 95-105.
9) Zhao L, Zhu X, Yu Y, et al. Comprehensive analysis of the anti-glycation effect of peanut skin extract. *Food Chem*. 2021; 362: 130169.
10) Venuprasad MP, Kandikattu HK, Razack S, et al. Chemical composition of *Ocimum sanctum* by LC-ESI-MS/MS analysis and its protective effects against smoke induced lung and neuronal tissue damage in rats. *Biomed Pharmacother*. 2017; 91: 1-12.
11) Kusindarta DL, Wihadmadyatami H, Haryanto A. The analysis of hippocampus neuronal density (CA1 and CA3) after *Ocimum sanctum* ethanolic extract treatment on the young adulthood and middle age rat model. *Vet World*. 2018; 11: 135-140.
12) Singleton VL, Orthofer R, Lamuela-Raventós RM. [14] Analysis of total phenols and other oxidation substrates and antioxidants by means of Folin-Ciocalteu reagent. *Methods Enzymol*. 1999; 299: 152-178.
13) Yao X, Zhu L, Chen Y, et al. *In vivo* and *in vitro* antioxidant activity and α-glucosidase, α-amylase inhibitory effects of flavonoids from *Cichorium glandulosum seeds*. *Food Chem*. 2013; 139: 59-66.
14) Hori M, Yagi M, Nomoto K, et al. Inhibition of advanced glycation end product formation by herbal teas and its relation to anti-skin aging. *Anti-Aging Med*. 2012; 9: 135-148.
15) Shin S, Son D, Kim M, et al. Ameliorating effect of *Akebia quinata* fruit extracts on skin aging induced by advanced glycation end products. *Nutrients*. 2015; 7: 9337-9352.
16) Takabe W, Yagi M, Ichihashi M, et al. Anti-glycative effect of palladium and platinum nanoparticle solution. *Glycative Stress Res*. 2016; 3: 222-228.
17) Sevindik HG, Ozgen U, Atila A, et al. Phytochemical studies and quantitative HPLC analysis of rosmarinic acid and luteolin 5-*O*-β-D-glucopyranoside on *Thymus praecox* subsp. grossheimii var. grossheimii. *Chem Pharm Bull (Tokyo)*. 2015; 63: 720-725.
18) Bhatarrai G, Seong SH, Jung HA, et al. Isolation and quantitative analysis of BACE1 inhibitory compounds from *Cirsium maackii* flower. *Nat Prod Sci*. 2019; 25: 326-333.
19) Ozgen U, Sevindik H, Kazaz C, et al. A new sulfated alpha-ionone glycoside from Sonchus erzincanicus Matthews. *Molecules*. 2010; 15: 2593-2599.
20) Flegkas A, Milosević Ifantis T, Barda C, et al. Antiproliferative activity of (–)-rabdosiin isolated from *Ocimum sanctum* L. *Medicines (Basel)*. 2019; 6: 37.
21) Moussaoui F, Zellagui A, Segueni N, et al. Flavonoid constituents from Algerian *Launaea resedifolia* (O.K.) and their antimicrobial activity. *Rec Nat Prod*. 2010; 4: 91-95.
22) D'Urso G, Masullo M, Seigner J, et al. LC-ESI-FT-MSn metabolite profiling of *Symphytum officinale* L. roots leads to isolation of comfreyn A, an unusual arylnaphthalene lignan. *Int J Mol Sci*. 2020; 21: 4671.
23) Zhou W, Xie H, Xu X, et al. Phenolic constituents from *Isodon lophanthoides* var. graciliflorus and their antioxidant and antibacterial activities. *J Funct Foods*. 2014; 6: 492-498.
24) Yagi M, Sakiyama C, Miyata Y, et al. Antiglycative effect of genipin and crocetin. *Glycative Stress Res*. 2021; 8: 156-161.
25) Yagi M, Nomoto K, Hori M, et al. The effect of edible purple Chrysanthemum extract on advanced glycation end products generation in skin: A randomized controlled clinical trial and *in vitro* study. *Anti- Aging Med*. 2012; 9: 61-74.
26) Takabe W, Yamaguchi T, Hayashi H, et al. Identification of antiglycative compounds in Japanese red water pepper (red leaf variant of the *Persicaria hydropiper* sprout). *Molecules*. 2018; 23: 2319.
27) Ohno R, Moroishi N, Sugawa H, et al. Mangosteen pericarp extract inhibits the formation of pentosidine and ameliorates skin elasticity. *J Clin Biochem Nutr*. 2015; 57: 27-32.
28) Rastogi S, Kalra A, Gupta V, et al. Unravelling the genome of Holy basil: An "incomparable" "elixir of life" of traditional Indian medicine. *BMC Genomics*. 2015; 16: 413.
29) Yang R, Wang WX, Chen HJ, et al. The inhibition of advanced glycation end-products by five fractions and three main flavonoids from *Camellia nitidissima* Chi flowers. *J Food Drug Anal*. 2018; 26: 252-259.
30) Rabbani N, Thornalley PJ. Dicarbonyl stress in cell and tissue dysfunction contributing to ageing and disease. *Biochem Biophys Res Commun*. 2015; 458: 221-226.
31) Takeuchi M, Makita Z. Alternative routes for the formation of immunochemically distinct advanced glycation end-products *in vivo*. *Curr Mol Med*. 2001; 1: 305-315.
32) Wu CH, Huang SM, Lin JA, et al. Inhibition of advanced glycation endproduct formation by foodstuffs. *Food Funct*. 2011; 2: 224-234.
33) Kim CS, Park S, Kim J, et al. The role of glycation in the pathogenesis of aging and its prevention through herbal products and physical exercise. *J Exerc Nutrition Biochem*. 2017; 21: 55-61.